Left hemisphere frontotemporal effective connectivity during semantic feature judgments: Differences between patients with aphasia and healthy controls

Erin L. Meier & Swathi Kiran
Sargent College of Health and Rehabilitation Sciences, Boston University

Introduction

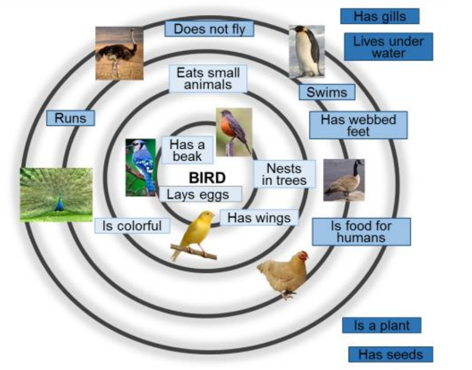

Figure 1. Schematic of category features in semantic space. Pale blue = typical, core features, medium blue = atypical, distinctive features, dark blue = out-of-category features

- Feature knowledge plays a critical role in the organization of the semantic system[1]
- Evidence from both healthy individuals and persons with stroke-induced aphasia (PWA) suggests correctly assigning or rejecting attributes to conceptual targets requires the integrated functioning of anatomically-remote areas spanning left frontotemporoparietal cortex[2-4], including:
  - Inferior frontal gyrus, pars triangularis (IFGtri) for semantic control[5-6]
  - Middle frontal gyrus (MFG) for domain-general cognitive-control[7-8]
  - Middle temporal gyrus (MTG) for multimodal lexical-semantic processing[2,9]
- However, little is known about the impact of stroke on the dynamic connectivity of such regions during semantic tasks

Study Aims

1. To examine frontotemporal effective connectivity for semantic judgments in PWA relative to controls using dynamic causal modelling (DCM)[10]
2. To examine the relationship between connectivity parameters, behavioral performance, and cortical integrity in PWA

Participants

- 18 controls (10M, mean age = 60.3 ± 10.9 years)
- 25 PWA (17M, mean age = 63.0 ± 11.0 years, mean months post onset [MPO] = 56 ± 53 months)
- Behavioral testing:
  - Western Aphasia Battery-Revised (WAB-R) to obtain an Aphasia Quotient (AQ), an overall index of aphasia severity, for each patient
  - Pyramids and Palm Trees Test (PPT) to assess nonverbal semantics
  - Psycholinguistic Assessments of Language Processing in Aphasia (PALPA), subtest 51: Word Semantic Association to assess lexical semantics for high and low imageable items

Table 1. Stroke and behavioral information for PWA

	MPO	Lesion Volume (cc)	WAB-R AQ	PPT %	PALPA51 High %	PALPA51 Low %
PWA1	12	74508	87.2	96.0	86.7	66.7
PWA2	13	92057	74.1	94.0	66.7	53.3
PWA3	8	172344	30.8	92.0	33.3	26.7
PWA4	113	324719	66.6	92.0	86.7	60.0
PWA5	137	210628	48.0	88.0	46.7	33.3
PWA6	37	11279	95.2	96.0	93.3	80.0
PWA7	12	68088	80.4	94.0	93.3	66.7
PWA8	104	210383	40.0	88.0	66.7	13.3
PWA9	18	8097	92.7	94.0	73.3	66.7
PWA10	24	59140	64.4	94.0	73.3	33.3
PWA11	62	130489	87.2	85.0	53.3	53.3
PWA12	71	321907	33.6	79.0	0.0	20.0
PWA13	152	159060	74.3	98.0	86.7	53.3
PWA14	152	154879	78.0	96.2	60.0	40.0
PWA15	23	87744	28.9	82.7	33.3	20.0
PWA16	20	257144	13.0	94.2	73.3	73.3
PWA17	164	235770	40.4	94.0	46.7	6.7
PWA18	33	136854	37.5	65.0	66.7	60.0
PWA19	115	89004	58.0	69.0	46.7	33.3
PWA20	22	111102	56.0	98.1	80.0	20.0
PWA21	49	79770	85.5	94.0	73.3	60.0
PWA22	12	57440	73.8	94.2	86.7	60.0
PWA23	18	13867	71.3	100.0	46.7	46.7
PWA24	13	56449	79.6	96.2	73.3	40.0
PWA25	21	5256	92.0	94.0	80.0	60.0
AVG	**56**	**125119**	**63.5**	**90.7**	**65.1**	**45.9**
STD DEV	**53**	**92683**	**23.5**	**8.6**	**22.4**	**20.3**

MRI Methods

- MR images acquired on a Siemens Trio TIM with a 20-channel head + neck coil
- T1 parameters: TR/TE = 2300/2.91ms, 176 sagittal slices, 1mm^3 voxels
- Functional parameters: TR/TE = 2570/30ms, 40 axial slices, interleaved with 2x2x3mm voxels
- fMRI task included 108 experimental stimuli (i.e., real pictures) and 36 scrambled control stimuli

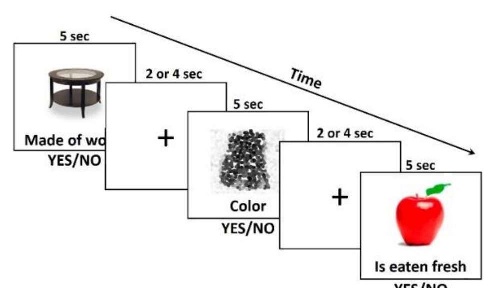

Figure 2. fMRI task. Example of event-related time series

Preprocessing
- Slice timing correction
- Realignment
- Coregistration:
  - Structural to mean functional image
  - Lesion mask and lesion map to PWA's structural image
- Segmentation
- Normalization
- Smoothing (4mm kernel)

→

Statistical Analysis
- 1st level GLM:
  - Modeled three conditions
  - Canonical HRF+TD
  - Contrast of interest: *pictures – scrambled*
- 2nd level analysis:
  - One-sample t-test in each group
  - Beta weights for each participant

→

% Spared Tissue
- Lesion masks manually drawn
- % spared tissue = (bounding region volume – normalized lesion volume) / (bounding region volume) in MarsBaR

Figure 3. Steps of MRI and fMRI analysis. Analysis completed in SPM12. Anatomically-constrained bounding regions of interest (ROIs) for spared tissue calculation created in the MarsBaR toolbox.

Effective Connectivity Methods: DCM

Volume of Interest (VOI) Selection

1. Peak maxima identified in each region from controls' 2nd-level analysis for *pictures – scrambled*, uncorr, p < .001 (see below)

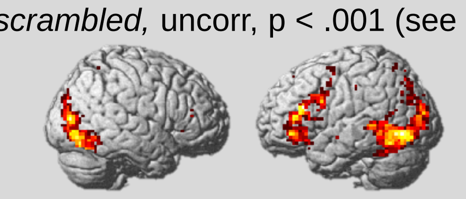

2. Anatomically-constrained bounding regions created to (1) ensure each subject's peak ≤ 35mm from control group peak and (2) to account for PWA's lesions

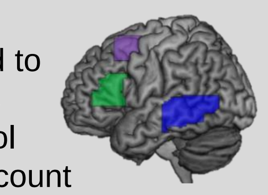

3. VOIs located and extracted for each subject per flowchart

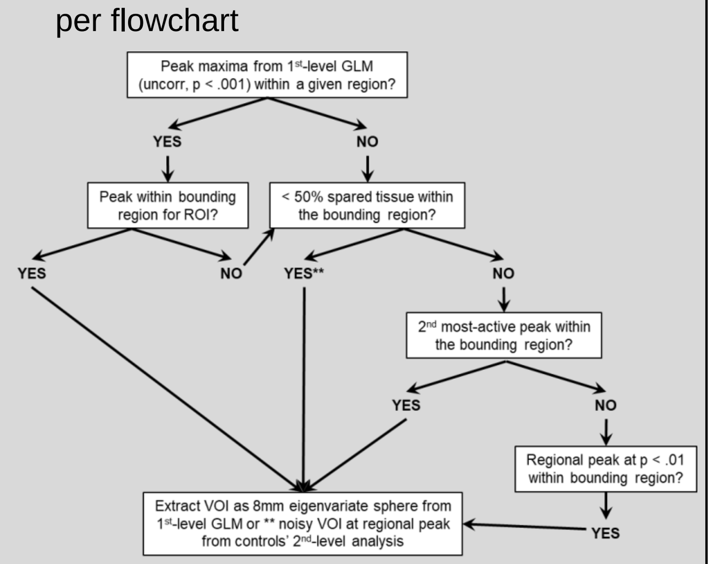

→

Model Specification & Estimation
- Bilinear, two-state, center input & non-stochastic models
- Fully inter-connected intrinsic connections (DCM-A)
- Effect of pictures modeled to regions (DCM-C) & connections (DCM-B)
- Model space partitioned into 3 families, with driving input to LIFG (Family #1), LMFG (Family #2) or LMTG (Family #3)

↓

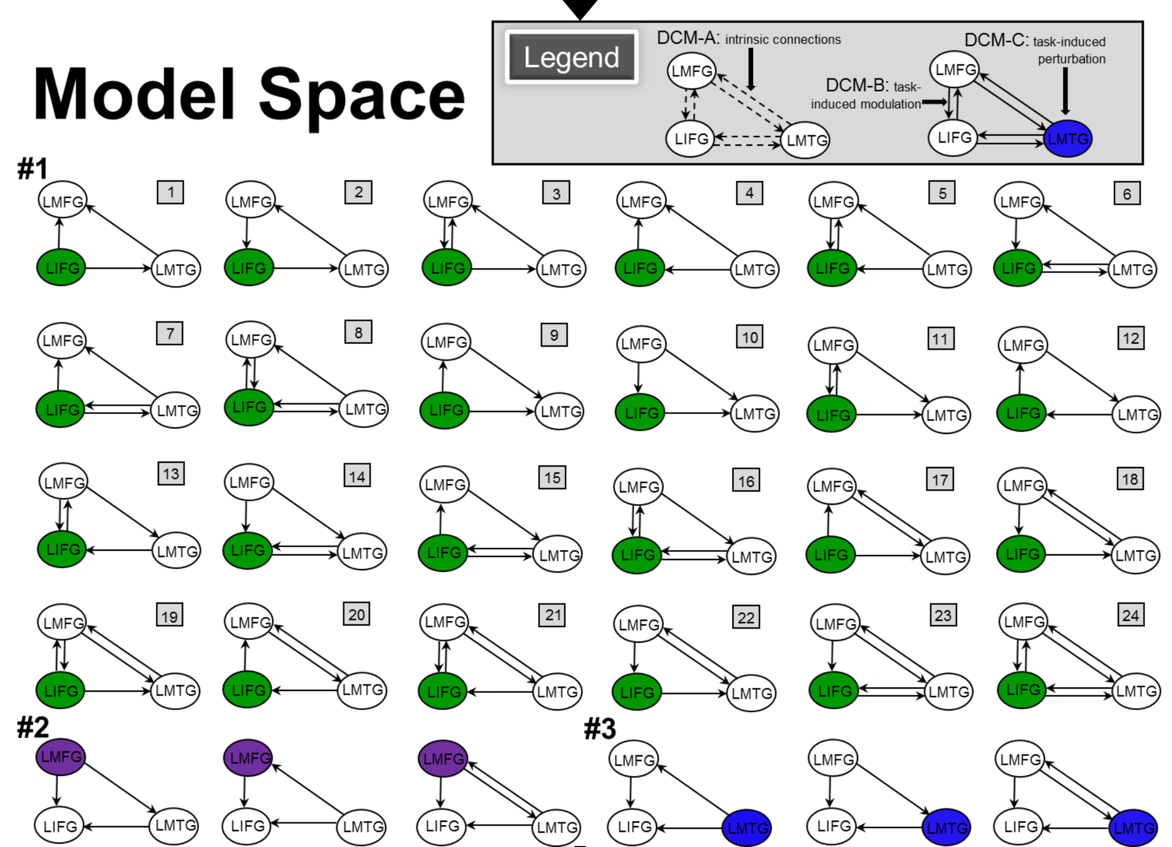

↓

Inference
- Family-wise Bayesian Model Selection (BMS) to determine which family of models best fit the data[11] = **Model inference**
- Bayesian Model Averaging (BMA) within each family to yield values reflecting connectivity in the absence of task (Ep.A), task-based modulation on connections (Ep.B), & task-induced perturbation to regions (Ep.C) = **Parameter inference**

Figure 4. Overview of effective connectivity (i.e., DCM) methods.

Results: VOI Integrity, Location, & Activation

Regional integrity in PWA

- LMTG and LMFG most damaged and spared regions, respectively
- Noisy VOIs (i.e., threshold @ p = 1.0 due to ≥ ~50% damage in bounding region) in LIFGtri and LMTG for three and five PWA, respectively

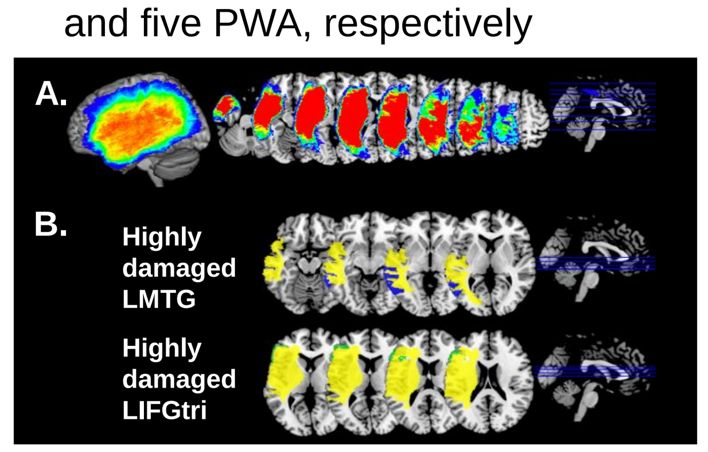

Figure 5. Lesion information. (A) Lesion overlay and (B) anatomically-constrained bounding regions for example PWA. Lesion (in yellow) subtracted from bounding region to yield remaining tissue in LMTG (in blue) for PWA2 and LIFG (in green) for PWA8

Table 2. Percent spared tissue

Patient	LIFGtri	LMFG	LMTG
PWA1	99.9	100.0	85.0
PWA2	100.0	100.0	36.3
PWA3	84.8	100.0	14.9
PWA4	15.9	68.2	11.4
PWA5	97.0	98.2	81.0
PWA6	100.0	100.0	100.0
PWA7	100.0	100.0	99.1
PWA8	34.5	100.0	85.8
PWA9	100.0	100.0	95.2
PWA10	77.9	95.6	87.1
PWA11	78.0	77.0	100.0
PWA12	36.0	28.0	11.0
PWA13	60.1	100.0	53.8
PWA14	84.3	100.0	52.5
PWA15	66.6	100.0	100.0
PWA16	2.6	98.5	42.8
PWA17	64.7	98.6	35.3
PWA18	95.2	100.0	65.6
PWA19	83.3	100.0	79.0
PWA20	71.4	100.0	25.7
PWA21	98.5	100.0	91.1
PWA22	100.0	100.0	41.6
PWA23	100.0	100.0	100.0
PWA24	98.2	100.0	100.0
PWA25	100.0	100.0	100.0
AVG	**78.0**	**94.6**	**67.8**

VOI location in PWA vs. controls

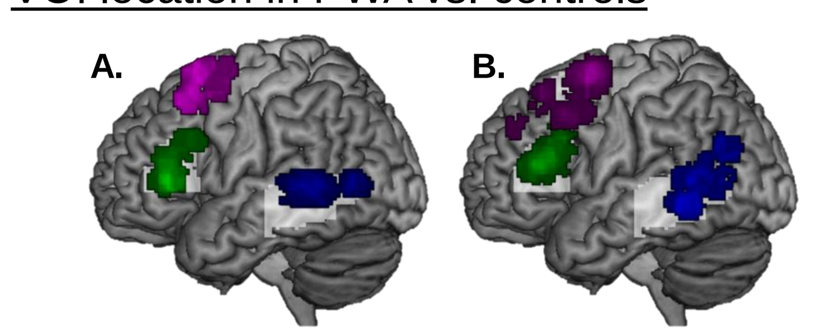

Figure 6. VOI location across all (A) controls and (B) PWA. White regions = Anatomically-constrained bounding regions

- No difference between groups in the location of individuals' VOIs for LIFG (t = -1.55, p = 0.13), LMFG (t = 0.93, p = 0.36) or LMTG (t = 0.62, p = 0.54)
- Mean distance from control group regional peaks:
  - LIFG: PWA=10.8 ± 3.0mm, Controls=12.9 ± 6.0mm
  - LMFG: PWA=20.1 ± 4.2mm, Controls=18.8 ± 6.7mm
  - LMTG: PWA=19.0 ± 3.0mm, Controls=16.0 ± 6.7mm

Strength of regional activity in PWA vs. controls

- No significant differences between groups in beta weights from anatomically-constrained bounding regions (F(1,40) = 1.01, p = 0.40)
- Provides some certainty that potential between-group differences in connectivity are *not* due to between-group differences in regional activity

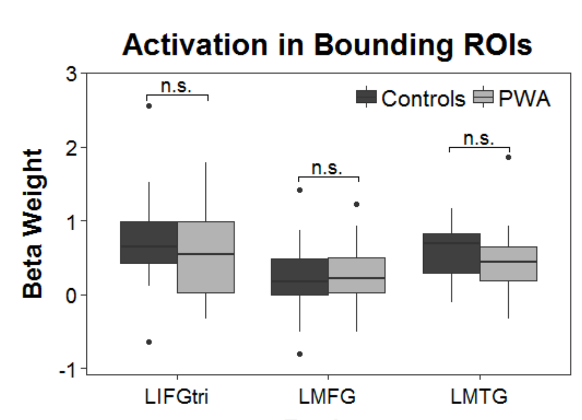

Figure 7. Activation in anatomically-constrained bounding regions per beta weights. n.s. = not significant

Results: DCM Model Inference

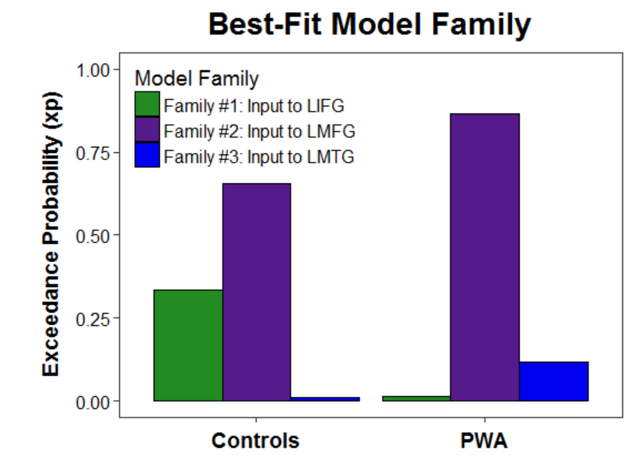

Figure 8. Family-wise BMS for each group

- Family #2: Input to LMFG was the best-fit model family for both groups
- For controls, however, model fit was mainly split between three individuals models:
  - One fully-connected bidirectional model from Family #1: Input to LIFG (i.e., model #24 [xp = 0.30])
  - Two highly-connected bidirectional models from Family #2: Input to LMFG (i.e., models #42 [xp = 0.25] and #48 [xp = 0.27])

Results: DCM Parameter Inference

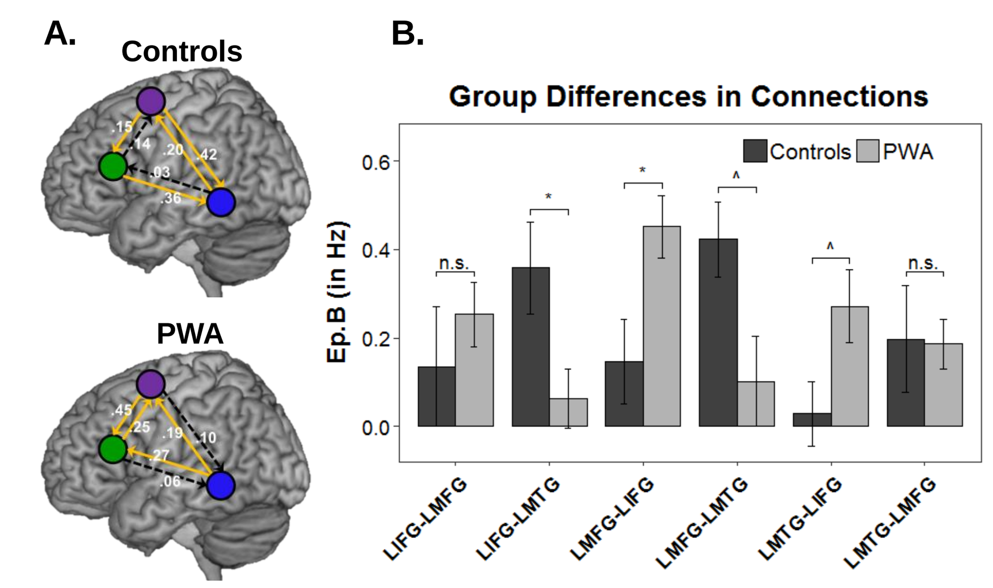

*Figure 9. Task-induced connection strength (Ep.B) in Hertz. (A) Significant connections within each group per one-sample t-tests. Solid yellow and dashed black lines indicate significant and non-significant connections, respectfully. (B) Differences in task-induced connections between PWA and controls. *p < .05, ^p = trending, n.s. = not significant*

- Significant connections within each group (Fig. 9A):
  - Controls: LIFG→LMTG, LMFG→LMTG, and bidirectional LMFG & LMTG connections
  - PWA: LMTG→LIFG, LMTG→LMFG and bidirectional LIFG & LMFG connections
- Overall difference between groups (F(1,40) = 2.43, p = 0.045) (Fig. 9B):
  - Controls > PWA for LIFG→LMTG (p = .02)
  - PWA > Controls for LMFG→LIFG (p = .01)

Relationships between connectivity, behavior, & VOI integrity in PWA

- No significant relationships between behavior and connectivity parameters
  - Lower accuracy on PALPA51 high imageability related to stronger LMTG activity (r = -0.51, p = 0.01)
- No significant relationships between regional activity in driving regions (e.g., LIFG in LIFG→LMTG) and connection strength (range: r = -0.27 – 0.47, p = 0.12 – 0.94)
- No significant relationships between integrity of driving regions and connection strength (range: r = 0.11 – 0.38, p = 0.39 – 0.60)

Conclusions

- When accounting for lesion in the patient group, all participants exhibited activation for semantic judgments in close proximity in each VOI
- Both groups demonstrated a preference for Family #2: Input to LMFG
- Regarding connections, controls demonstrated top-down modulation of LMTG by frontal regions, which suggests semantic and cognitive control processes are at play during successful semantic decisions[5-6,8]
- PWA demonstrated high reliance on interactions between LMFG and LIFG[12-13] and modulation of frontal areas by LMTG
  - Network differences possibly due to interactions with other areas, including right hemisphere homologues of VOIs

Selected References

1. Rosch, E., & Mervis, C. B. (1975). Family resemblances: Studies in the internal structure of categories. *Cognitive Psychology*, *7*, 573–605. doi:10.1016/0010-0285(75)90024-9
2. Binder, J. R., Desai, R. H., Graves, W. W., & Conant, L. L. (2009). Where is the semantic system? A critical review and meta-analysis of 120 functional neuroimaging studies. *Cerebral Cortex*, *19*(12), 2767-2796. doi:10.1093/cercor/bhp055 [doi]
3. Vigneau, M., Beaucousin, V., Hervé, P. Y., Duffau, H., Crivello, F., Houdé, O., Mazoyer, B., & Tzourio-Mazoyer, N. (2006). Meta-analyzing left hemisphere language areas: Phonology, semantics, and sentence processing. *NeuroImage*, *30*, 1414-1432.
4. Turkeltaub, P. E., Messing, S., Norise, C., & Hamilton, R. H. (2011). Are networks for residual language function and recovery consistent across aphasic patients? *Neurology*, *76*(20), 1726-1734. doi:10.1212/WNL.0b013e31821a44c1 [doi]
5. Thompson-Schill, S. L., D'Esposito, M., Aguirre, G. K., & Farah, M. J. (1997). Role of left inferior prefrontal cortex in retrieval of semantic knowledge: A reevaluation. *Proceedings of the National Academy of Sciences of the United States of America*, *94*(26), 14792-14797.
6. Whitney, C., Kirk, M., O'Sullivan, J., Lambon Ralph, M. A., & Jefferies, E. (2011). The neural organization of semantic control: TMS evidence for a distributed network in left inferior frontal and posterior middle temporal gyrus. *Cerebral Cortex*, *21*(5), 1066-1075. doi:10.1093/cercor/bhq180 [doi]
7. de Zubicaray, G., Zelaya, F., Andrew, C., Williams, S., & Bullmore, E. (2000). Cerebral regions associated with verbal response initiation, suppression and strategy use. *Neuropsychologia*, *38*(9), 1292-1304.
8. Fedorenko, E., Duncan, J., & Kanwisher, N. (2013). Broad domain generality in focal regions of frontal and parietal cortex. *Proceedings of the National Academy of Sciences*, *110*(41), 16616–16621.
9. Visser, M., Jefferies, E., Embleton, K. V., & Ralph, M. A. L. (2012). Both the middle temporal gyrus and the ventral anterior temporal area are crucial for multimodal semantic processing: Distortion-corrected fMRI evidence for a double gradient of information convergence in the temporal lobes. *Journal of Cognitive Neuroscience*, *24*(8), 1766-1778.
10. Friston, K. J., Harrison, L., & Penny, W. (2003). Dynamic causal modelling. *Neuroimage*, *19*(4), 1273-1302.
11. Penny, W. D., Stephan, K. E., Daunizeau, J., Rosa, M. J., Friston, K. J., Schofield, T. M., et al. (2010). Comparing families of dynamic causal models. *PLoS Computational Biology*, *6*(3), e1000709. doi:10.1371/journal.pcbi.1000709 [doi]
12. Meier, E. L., Kapse, K. J., & Kiran, S. (2016). The relationship between frontotemporal effective connectivity during picture naming, behavior, and preserved cortical tissue in chronic aphasia. *Front. Hum. Neurosci.*, *10*, 109. DOI: 10.3389/fnhum.2016.00109.
13. Geranmayeh, F., Chau, T. W., Wise, R. J., Leech, R., & Hampshire, A. (2017). Domain-general subregions of the medial prefrontal cortex contribute to recovery of language after stroke. *Brain*, *140*(7), 1947-1958.

Acknowledgments

We would like to thank all the individuals who participated in this project. Additionally, we extend our thanks to members of the BU Aphasia Research Lab for their assistance with data collection and analysis. This study was supported by NIH/NIDCD grant 1P50DC012283 and the Center for the Neurobiology of Language Recovery. Research, training, and travel support was additionally provided by NIH/NIDCD grant F31DC015940.